Spin-resolved inverse-photoemission study of Ni(001) and its chemisorption

Leonard E. Klebanoff,* Robert K. Jones, Daniel T. Pierce, and Robert J. Celotta
National Bureau of Standards, Gaithersburg, Maryland 20899
(Received 15 June 1987)

Results from an angle-resolved spin-polarized inverse photoelectron spectroscopy (ARSPIPES) study of Ni(001), $c(2\times2)$O/Ni(001), and $c(2\times2)$S/Ni(001) are presented. Inverse-photoemission spectra for the clean Ni(001) surface are in good agreement with previous work. A minority-spin character is found for a direct radiative transition into an unoccupied 3*d* band. No definitive spin dependence is found for radiative transitions into the unoccupied 4*sp* band, a potentially unresolved crystal-induced surface state, or an image-potential surface state. A chemisorbed $c(2\times2)$ oxygen overlayer does not appreciably affect the measured spin dependence or spectral intensity of the Ni 3*d* radiative transition. Little evidence is found for an oxygen-induced unoccupied state above the Fermi level at the $\bar{\Gamma}'$ point of the surface Brillouin zone. The persistent spin asymmetry for the Ni 3*d* transition suggests that any magnetization decrease induced by oxygen is probably confined to the Ni surface layer. In contrast to $c(2\times2)$O/Ni(001), a $c(2\times2)$ sulfur overlayer increases the spectral intensity just above the Fermi level, and drastically reduces the measured spin dependence of the ARSPIPES spectra. These observations are tentatively assigned to a sulfur-induced majority-spin state above the Fermi level at $\bar{\Gamma}'$. The image-potential state remains fixed in energy upon $c(2\times2)$ sulfur chemisorption. This behavior is in contrast to that observed for $c(2\times2)$O/Ni(001), and indicates that the Ni(001) image-potential state energy need not shift with adsorbate-induced variations in the work function.

I. INTRODUCTION

The 3*d*-electron states in nickel are thought to be quite atomiclike,[1] and screen the nuclear charge rather poorly. Relative to the 3*d* electrons of elements with lower atomic number, the 3*d* electrons in Ni experience a large effective nuclear charge. Consequently, the calculated[2] radial extent ($\lesssim 0.75$ Å) of the 3*d* atomic wave function is small compared with the nearest-neighbor distance in Ni (2.49 Å). The lattice potential does not affect the 3*d* orbitals in Ni as much as the 4*s* and 4*p* valence orbitals.[1] The result of these factors is a localization of the 3*d* valence electronic structure, and a concomitant narrowing of the valence electron bandwidth. The narrowed bandwidth favors the correlated motion of the 3*d* valence electrons. Two spectroscopic manifestations of electron correlation in nickel are valence-band and core-level photoelectron satellites.[3–7] Such satellites are very prominent in nickel and have been extensively explored with photoelectron spectroscopy.[6,7] A third manifestation of electron correlation is perhaps the most important—magnetism. The magnetic, electronic, and chemical properties of ferromagnetic Ni(001) are the subjects of this angle-resolved spin-polarized inverse photoelectron spectroscopy (ARSPIPES) investigation.

The technique ARSPIPES reveals the spin dependence of surface and near-surface unoccupied electronic structure in a wave-vector-resolved manner.[8] This permits a direct investigation of the quantum mechanical basis for magnetism, i.e., the spin-dependent energy band structure. Nickel has been a particularly suitable system for ARSPIPES,[8–10] since its unoccupied 3*d* band structure is believed to be completely of minority-spin character. The spin dependence of the unoccupied electronic structure of clean Ni(001) is the initial topic of this paper.

The unoccupied band structure of nickel surfaces are thought to determine in part their chemical reactivity. This band structure[11–13] and its variation with oxygen chemisorption[14–17] has been the subject of several inverse photoemission (IP) studies of nickel surfaces. The (001) face is a particularly attractive surface for further experimentation. Although historically controversial,[18] the geometric structure of a $c(2\times2)$ oxygen overlayer on Ni(001) is now thought to be known. With this structural information, theorists have been able to make extensive and detailed predictions for the electronic structure of $c(2\times2)$O/Ni(001).[19–26] To understand more fully the effect of a chemisorbed $c(2\times2)$ oxygen layer on the magnetic and unoccupied electronic structure of Ni(001), we also present here results from an ARSPIPES study of $c(2\times2)$O/Ni(001).

The chemisorption of sulfur on Ni(001) has been far less controversial from a structural point of view.[27,28] However, comparatively few theoretical predictions have been made for the $c(2\times2)$S/Ni(001) system.[29–31] This fact is particularly surprising given the importance of sulfur in poisoning commercial catalysts. Angle-resolved photoelectron spectroscopy measurements[30] have provided information on the occupied electronic structure of $c(2\times2)$S/Ni(001). However, no information has been available on the unoccupied valence-band structure. To investigate the magnetic and electronic consequences of sulfur chemisorption on a clean Ni(001) surface, we have also conducted an ARSPIPES study of $c(2\times2)$S/Ni(001). It will be seen that $c(2\times2)$ oxygen and $c(2\times2)$ sulfur have very different effects on the sur-

face and near-surface magnetism and electronic structure of Ni(001).

The remainder of this paper is organized as follows. The experimental details will be described in Secs. II and III. In Secs. IV–VI, results will be presented and discussed from our ARSPIPES studies of clean Ni(001), $c(2\times2)$O/Ni(001), and $c(2\times2)$S/Ni(001), respectively. Conclusions are summarized in Sec. VII.

II. EXPERIMENTAL

The experimental geometry for our ARSPIPES measurements is shown in Fig. 1. Electrons with 27%±3% [27(3)%] spin polarization are emitted from a negative electron affinity GaAs source.[32] These electrons are directed onto the Ni(001) sample at an angle θ_e from the [001] surface normal in the (100) mirror plane (defined by the [001] and [010] axes). The quantization axis of the electron spin was adjusted to be parallel or antiparallel to the $[0\bar{1}0]$ magnetization axis of the sample, as shown in Fig. 1. Photons of energy 9.7 eV are generated via inverse photoemission at the sample, and detected with a He-I_2 Geiger-Müller tube.[33] All of the reported spectra were collected using a CaF_2 window as the high-energy cutoff. This cutoff, combined with the photoionization onset of I_2, provides an instrumental energy bandpass of 0.7 eV FWHM centered at 9.7 eV. Occasionally, a SrF_2 cutoff window was used. This window improved the energy resolution to 0.5 eV FWHM, and shifted the mean of the detected photon energy to 9.5 eV (Ref. 11). The increased spectral resolution, at the cost of significant signal, did not appreciably enhance the information content of the spectra. All ARSPIPES spectra were recorded by varying the kinetic energy of the incident electron beam. Experimental angles are accurate to within ±1°. The divergence of the incident electron beam is estimated to be ±3° (Ref. 8).

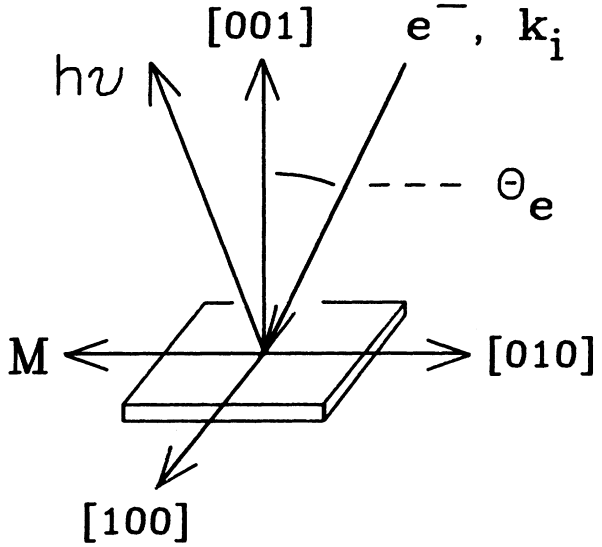

FIG. 1. The experimental geometry. The Ni(001) sample is magnetized along the $[0\bar{1}0]$ direction, as indicated by the vector **M**. Spin-polarized electrons are directed onto the sample at an angle θ_e from the [001] normal in the (100) mirror plane.

Our sample was a high-purity nickel crystal that was cut and oriented to within ±0.1° of the (001) plane, and mechanically polished (0.5 μm diamond paste) to a mirror finish. The sample was cleaned *in situ* by prolonged ($\approx$2 h) heating of the crystal at 973 K in 1×10^{-7} Torr of oxygen. This procedure removed surface and subsurface carbon, but left a surface oxide layer. The oxide layer was removed by annealing the crystal at 1023 K in 1×10^{-6} Torr of hydrogen for 90 min. After this initial treatment, the crystal was cleaned by argon-ion bombardment (4×10^{-6} Torr, 1.0 kV) for $\approx$1 h, followed by an anneal to 973 K. Occasionally, 1 langmuir (1 langmuir = 1 L $\equiv 1\times10^{-6}$ Torr sec) of oxygen was admitted before the anneal to burn off residual carbon. Typical contamination (S, C, and O) levels were less than 0.02 monolayers total, as measured with Auger electron spectroscopy.

After one hour exposure to the residual gases in our chamber (operating pressure $=2\times10^{-10}$ Torr), the crystal surface became contaminated with adsorbed carbon monoxide (CO). Flashing the crystal to 973 K for 3 min. removed virtually all of this adsorbed CO. Frequent flashing of the crystal in this manner permitted relatively uninterrupted study of the clean surface for $\approx$5 h. At the end of this time, the crystal was argon-ion bombarded for one hour to remove accumulated impurities. The crystal was then annealed at 973 K for 5 min to restore order to the clean surface.

The sample was mounted on a horseshoe iron electromagnet and magnetized along the $[0\bar{1}0]$ direction, as indicated in Fig. 1. *In situ* magneto-optic Kerr-effect measurements indicated that the crystal could not be remanently magnetized. We therefore magnetized our sample by applying 0.75 A to the windings of the electromagnet. From Kerr-effect measurements, we estimate the induced magnetization to be 35(5)% of saturation. This incomplete magnetization, the uncertainty in the spin polarization of the electron source, and the unknown magnetic anisotropy of the Ni(001) surface limit the quantitative polarization information obtainable from any single spin-resolved spectrum. However, comparisons between ARSPIPES spectra are much more quantitative.

Stray magnetic fields from the iron electromagnet produced vertical deflections of our low-energy incident electron beam. By observing the field-induced energy shifts of Ni(001) IP spectral peaks with known angle-dependent energy dispersions, we estimate this deflection to be 14° from the surface normal. This deflection was present only for the spin-resolved measurements on magnetized samples.

A $c(2\times2)$O/Ni(001) sample was prepared by exposing a clean Ni(001) surface at 298 K to 20 L of oxygen, followed by an anneal to 473 K for 3 min. This produced a clear $c(2\times2)$ low-energy electron diffraction (LEED) pattern. A $c(2\times2)$S/Ni(001) sample was made by exposing a clean Ni(001) surface at 298 K to 20 L of H_2S, followed by an anneal to 523 K. The LEED pattern for $c(2\times2)$S/Ni(001) was particularly sharp. Gas purities were monitored with a residual gas analyzer.

For both oxygen and sulfur, the ARSPIPES spectra were identical for annealed and unannealed samples. In this regard, we note that the anneals following gas adsorption did not significantly improve the visual quality of the already clear $c(2\times2)$O/Ni(001) and S/Ni(001) LEED patterns.

At lower gas exposures, we found no visual evidence for the quarter-monolayer $p(2\times2)$ LEED patterns found previously[18] for the O/Ni(001) and S/Ni(001) systems. Occasionally, these patterns were observed at the extreme edges of our Ni crystal. While this puzzling result does not directly affect the $c(2\times2)$ results presented here, we speculate that for our sample the $c(2\times2)$ half-monolayer structures developed from smaller $c(2\times2)$ adsorbate clusters on the Ni(001) surface.

The photon detector counts $n_\uparrow$ and $n_\downarrow$ were recorded in two separate channels, for the incident spin direction parallel to the majority- and minority-spin directions in the Ni crystal, respectively. The spin-dependent asymmetry (in percent), A, in the photon production is defined as[8]

$$A \equiv \frac{N_\uparrow - N_\downarrow}{N_\uparrow + N_\downarrow} \times 100 = \frac{n_\uparrow - n_\downarrow}{P_0(n_\uparrow + n_\downarrow)} \times 100 \ . \quad (1)$$

The factor P_0 accounts for the fact that the polarization of our electron source is less than 100% ($P_0 < 1$). The photon counts $N_\uparrow$ and $N_\downarrow$ are the number of photons that would be detected for a 100% spin-polarized electron beam, polarized parallel and antiparallel to the majority-spin direction, respectively. The statistical uncertainty ΔA (one standard deviation) is given approximately for the normal incidence geometry by $\Delta A = 1/[P_0(n)^{0.5}]$, where $n = n_\uparrow + n_\downarrow$ and P_0 is the magnitude of the electron source polarization $P_0 = 0.27(3)$.

III. QUESTIONS OF NORMALIZATION

By normalizing a spectral intensity we attempt to correct data for known or measured causes of intensity variation that are external to the physical system being investigated. Sources of photon intensity variation in our experiment are the electron current incident on the Ni(001) sample, and the Geiger-Müller photon detector sensitivity. Ideally, one would like to monitor and normalize for both of these variables. The current absorbed by the sample may at first seem to be an indicator of the incident electron current. However, as shown in Fig. 2, the current absorbed by the sample varied smoothly as a function of energy above the Fermi level E_F. The total change in absorbed current from E_F to 6 eV above E_F is $\approx 27\%$ for clean Ni(001). This variation in absorbed current could have both intrinsic and extrinsic causes. Causes intrinsic to the sample could be changes in the elastic or inelastic scattering processes with electron kinetic energy. An external cause could be stray magnetic fields that deflect the low-energy portion of our electron beam. Since these variations are neither known nor measured, we do not normalize the spectral intensity within a given IP spectrum to the absorbed current. We

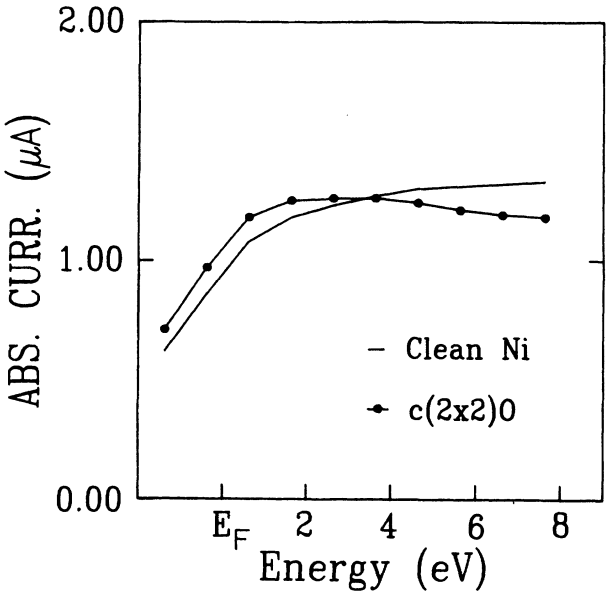

FIG. 2. The variation of the absorbed current with energy for clean Ni(001) (solid line) and $c(2\times2)$O/Ni(001) (dotted line). The energy scale for the figure is that appropriate for an inverse photoemission spectrum, i.e., the energy reported is the final-state energy above E_F if the electron had made a 9.7-eV radiative transition.

therefore choose not to make highly quantitative claims regarding the relative photon intensities within a given spectrum.

Several figures in this paper will compare IP spectra for a given sample recorded at various electron incidence angles θ_e. These spectra were normalized to each other via measurements of the IP count rate at normal incidence ($\theta_e = 0°$) for an electron energy 7.6 eV above E_F (a featureless part of the IP spectrum). This one-point normalization procedure ensures a proper correction for the small ($\approx 2\%$) drifts in the electron source emission (and therefore in the incident electron current), as well as the larger ($\approx 20\%$) variations in the Geiger-Müller detector sensitivity. This normalization process will be referred to as procedure A.

The problem of normalization is severe in comparing spectra of different physical systems, in our case clean versus chemisorbed Ni(001). The one-point normalization procedure A described above cannot be used, since the IP count rate at a given energy and angle can vary with chemisorption. Furthermore, the absorbed current at a particular point is not a suitable normalization standard. As shown in Fig. 2, the current absorbed by the nickel sample changes considerably when a $c(2\times2)$ oxygen overlayer is formed. Similar results were observed for $c(2\times2)$S/Ni(001). This variation probably results from adsorbate-induced variations in elastic and inelastic electron scattering processes. Such processes are intrinsic to the sample and are not characterized. We therefore choose to normalize the spectra at the unoccupied $3d$ energy to the *incident* electron current, whose stabili-

ty is monitored via the total GaAs source emission current. Normalization for drifts in the photon detector sensitivity were also made by monitoring the detector's response to blackbody photons emitted from a nearby ionization gauge. We call this normalization process procedure B. The overall accuracy of such normalizations was measured to be $\pm 10\%$.

IV. RESULTS AND DISCUSSION: CLEAN Ni(001)

Figure 3 presents a spin-integrated IP spectrum of clean Ni(001) taken in normal incidence ($\theta_e = 0°$). Three distinct spectral features are observed. The spectral features 1 [0.37(7) eV] and 2 [1.28(7) eV] have been previously assigned[11–13] to direct radiative transitions from an initial ground-state unoccupied bulk conduction band to unoccupied $3d$ and $4sp$ states, respectively. It has also been suggested[34,35] that feature 2 may originate from transitions into both a bulklike Ni $4sp$ band and a nearly degenerate crystal-induced surface state. Indirect evidence for this assignment will soon be presented.

In the presence of inelastic processes,[36] the initial-state band dispersion in Ni may be modified from a ground-state conduction band[37] toward the dispersion of a free electron as indicated by the dotted line in Fig. 4. The true initial-state band dispersion probably lies between these two extremes. For the free-electron band we have a $k_\perp(\text{Å}^{-1})$ dispersion[38]

$$k_\perp = 0.512(E_{\text{kin}} + V_0)^{1/2} . \quad (2)$$

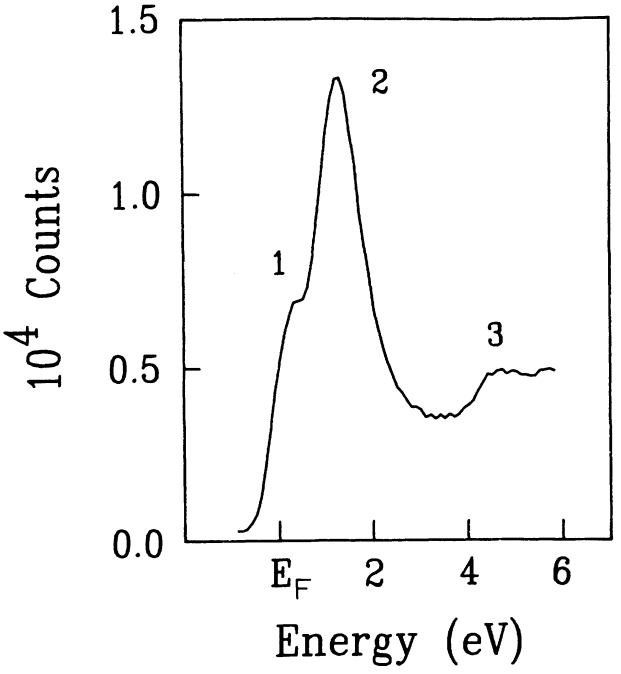

FIG. 3. A normal incidence ($\theta_e = 0°$) spin-integrated IP spectrum of clean Ni(001). The energy reported is the final-state energy above E_F of an electron making a 9.7-eV radiative transition. The sample was demagnetized prior to data collection.

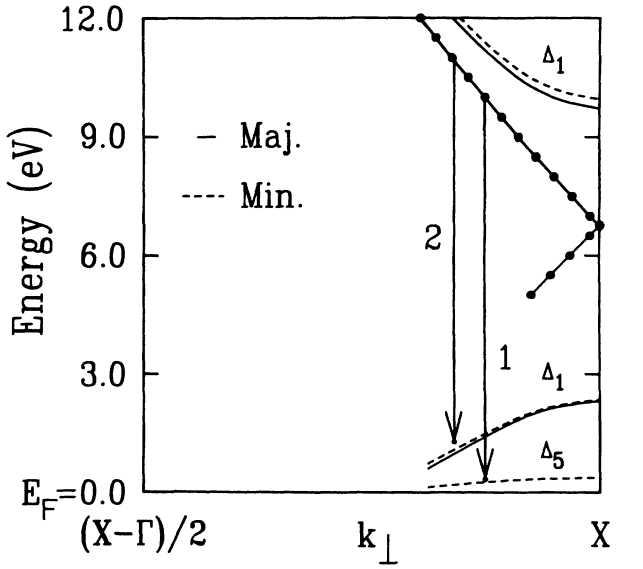

FIG. 4. The $k_\perp$ assignment of the radiative transitions 1 and 2 along the [001] Γ-X line near X. The solid and dashed lines are the unoccupied Ni majority-spin and minority-spin $E(k)$ relations, respectively, predicted by Fuster and Callaway (Ref. 37). Only Δ_1 and Δ_5 symmetry bands are plotted. The dotted line is a free electron dispersion relation using an inner potential of 10.4 eV [see Eq. (2) of text]. The length of the vertical arrows 1 and 2 corresponds to 9.7 eV.

Here, E_{kin} is the kinetic energy (in eV, relative to the vacuum level) of the incident electron that produces a spectral peak. The term V_0 (eV) is the "inner potential" energy that represents the attractive exchange-correlation energy felt by an electron within the solid. For V_0 we use the value 10.4 eV derived from the Ni(001) normal-emission angle-resolved photoemission study of Eberhardt and Plummer.[39] With the free-electron band of Eq. (2), a $k_\perp$ value can be assigned to an incident electron with energy E_{kin}. Figure 4 shows that for the initial-state energies (with respect to $E_F = 0$ eV) observed for the spectral features 1 and 2, $k_\perp$-conserving and energy-conserving 9.7-eV transitions can take place from the free-electron band to the calculated[37] unoccupied Ni electronic structure. Thus, the free-electron initial state described by Eq. (2) provides an excellent account of the radiative transitions 1 and 2 both in terms of energy and wave vector conservation. It is interesting that Eq. (2) also accurately accounts for angle-resolved photoemission[39] from Ni(001). Due to the finite energy and wave vector resolution of the IP measurement, the elucidation of the true nature of the inverse photoemission initial state is beyond the scope of the present study.

The spectral feature 3 [4.70(7) eV] has been assigned to transitions into a bound state induced by the Ni(001) surface image potential.[35,40] This type of state arises from the repeated total reflection of an electron between the crystalline potential and the surface image-potential barrier.[35,40–42] Since the details of the image-potential barrier are thought to determine the energy of this state,

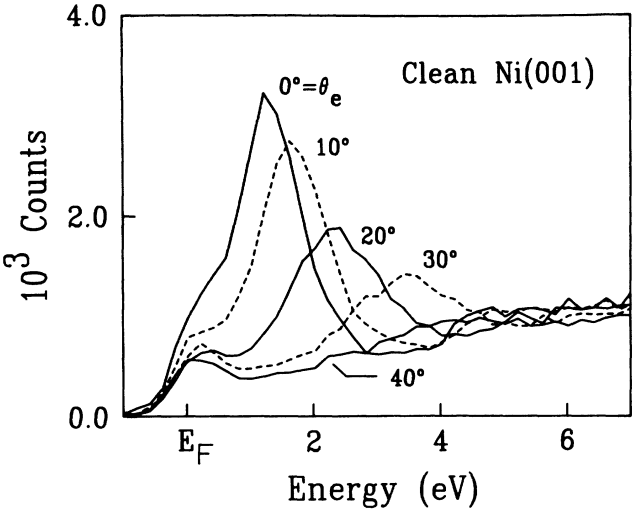

FIG. 5. The variation of clean Ni(001) spin-integrated IP spectra with electron incidence angle θ_e. The angle θ_e is varied in the (100) mirror plane. The spectral intensities are normalized using procedure A (see Sec. III). The sample was demagnetized prior to data collection.

the bound state is called an "image-potential" or "barrier-induced" surface state.

Figure 5 reveals the variation of the IP spectra as the incident electron angle θ_e is increased in the (100) mirror plane. These spectra were normalized to each other using procedure A. As θ_e increases, feature 1 loses intensity, but remains stationary in energy. Both the peak-2 and the image-potential state 3 lose intensity with angle, and disperse to higher energy. The results of Fig. 5 are in excellent agreement with the previous work of Goldmann *et al.*[11]

Figure 6 presents results from an ARSPIPES measurement of clean Ni(001). *We observe a* $-10(2)\%$ *spin asymmetry for the spectral feature 1.* This confirms the previous assignment[11–13] of this peak to a minority-spin 3*d* band. *No definitive spin asymmetry is found for the spectral peak 2,* as shown in Fig. 6. This lack of spin asymmetry is consistent with a 4*sp* assignment of this spectral band. One would not expect a sizeable spin dependence (or magnetization) for the large bandwidth 4*sp* band. No evidence is found for a spin splitting of the 4*sp* band like that observed previously[43] for Ni(011). It should be remembered that peak 2 may include spectral intensity from an unresolved crystal-induced surface state.

Figure 7 presents an ARSPIPES spectrum of feature 3. The spin asymmetries observed in Fig. 7 are rather small and show statistical scatter. However, it is clear from Fig. 7 that the spectral intensity associated with peak 3 decreases the spin asymmetry of the ARSPIPES spectrum. A careful analysis of the spin asymmetry data suggests that *the image-potential state 3 adds spin-independent intensity to the ARSPIPES spectrum,* to within the experimental error. The spin independence of the barrier-induced state 3 is easily rationalized. The band gap in which the surface feature 3 is located is theoretically independent of electron spin. Also, state 3 is thought to be a barrier-induced state, with most of the amplitude of the associated wave function residing well outside the surface layer in the vacuum.[44] Since the exchange interaction depends on the overlap of electron orbitals centered on the same or nearest-neighbor sites, it is not too surprising that a negligible exchange interaction is experienced by an electron in the Ni(001) image-potential surface state. If there were an intrinsic spin dependence of peak 3, that dependence might be small since even for bulk nickel, the exchange splitting 0.3 eV

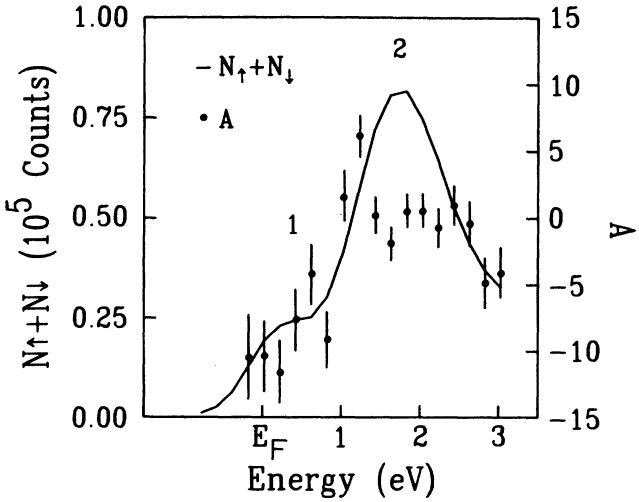

FIG. 6. A spin-integrated, nominally normal incidence (see Sec. II) IP spectrum (solid line) of clean Ni(001) magnetized along the [0$\bar{1}$0] direction. Also plotted is the measured spin asymmetry A [in percent, see Eq. (1) in text] for the spectral features 1 and 2. The error bars on A (in percent) were calculated using the formula given in Sec. II.

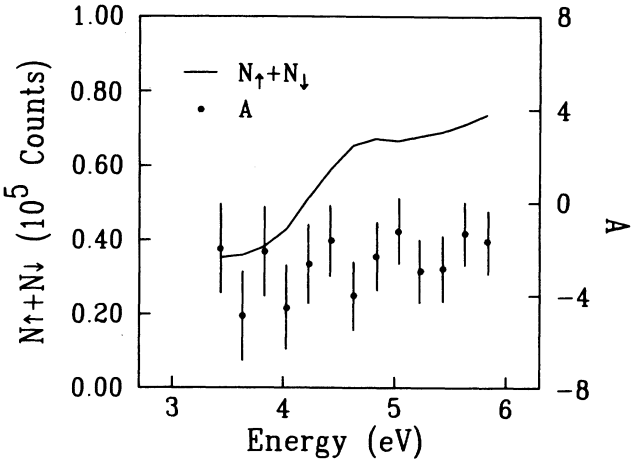

FIG. 7. A spin-integrated, nominally normal incidence (see Sec. II) IP spectrum (solid line) of the surface feature 3. Also plotted is the measured spin asymmetry (in percent) A for feature 3. The error bars on A (in percent) were calculated using the formula given in Sec. II.

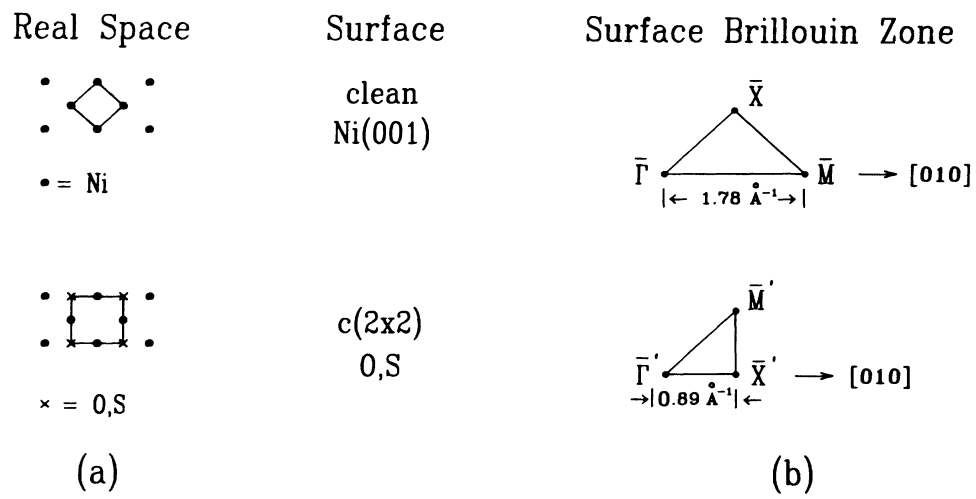

FIG. 8 (a) A top view of the clean Ni(001) surface, and a Ni(001) surface with $c(2\times2)$ chalcogen overlayer. (b) The surface Brillouin zones (SBZ) for clean Ni(001), and for a Ni(001) surface with a $c(2\times2)$ oxygen or sulfur overlayer.

is not very large. These factors, combined with the modest energy resolution of our measurement, probably conspire to produce a negligible spin dependence of the direct radiative transition 3 to the image-potential surface state. It would be interesting to investigate the spin dependence of an image-potential state on ferromagnetic iron, for which the exchange splitting is ≈ 2 eV.

V. RESULTS AND DISCUSSION: $c(2\times2)$O/Ni(001)

The chemisorption of oxygen on Ni(001) has been a controversial topic, both in terms of adsorbate geometric and electronic structure.[18] This is due in part to the competition between chemisorption and oxidation at any given coverage. Throughout the range of exposures over which a $c(2\times2)$ LEED pattern is observed, the relative amounts of oxide and chemisorbed oxygen can vary considerably.[18] It has been previously argued that the oxygen overlayer is predominantly chemisorbed just after the initial steep rise in the oxygen uptake curve.[18] In our experiments, this point corresponded to an exposure of 20 L. It is this chemisorbed $c(2\times2)$ oxygen overlayer that is the subject of this study. Figure 8(a) displays a top view of a clean Ni(001) surface, and a Ni(001) surface with a $c(2\times2)$ chalcogen half monolayer. The relevant surface Brillouin zones (SBZ) for each are shown in Fig. 8(b).

Figure 9 presents a comparison of normal-incidence IP spectra of clean Ni(001) (solid line) and $c(2\times2)$O/Ni(001) (dots). These spectra have been normalized at the 3*d* energy using procedure B. Note the substantial decrease in the intensity of the direct transition 2, with little change in the peak-2 energy. In contrast with previous IP results[14,15] we observe a small decrease in the spectral intensity at the 3*d* feature 1. This decrease could be largely attributable to the intensity decrease of the nearby spectral peak 2, because of the modest energy resolution of the experiment. *Spin-resolved measurements of feature 1 for* $c(2\times2)O/Ni(001)$ *reveal a* $-9(2)\%$ *spin asymmetry.* This is the same spin dependence (to within the experimental error) that was observed for this feature on the clean surface.

The surface feature 3 decreases in intensity somewhat with chemisorbed oxygen and shifts to higher energy by $\approx 0.47(7)$ eV. The Ni(001) work function ($\phi_{Ni}=5.0$ eV) is reported to increase by 0.36 eV with $c(2\times2)$ oxygen chemisorption.[45] The observed energy shift for the image-potential state is thus qualitatively consistent with the view[46] that the energies of image barrier-induced states track adsorbate-induced variations in the work function. The angular dependence of the $c(2\times2)$O/Ni(001) IP is shown in Fig. 10. The 3*d* band

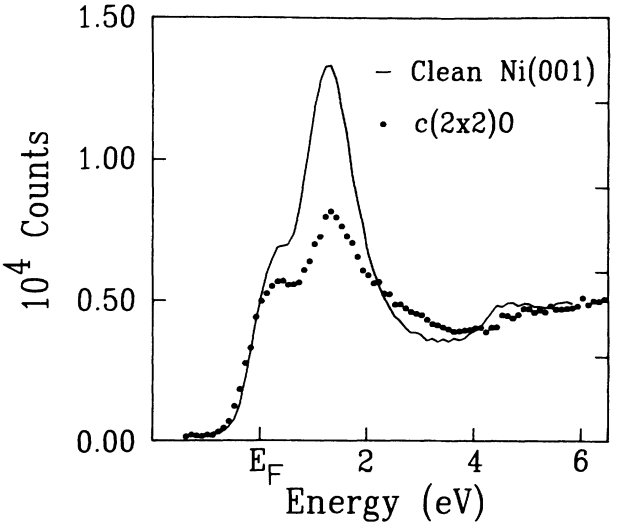

FIG. 9. A comparison of normal incidence ($\theta_e=0°$) spin-integrated IP spectra of clean Ni(001) (solid line) and $c(2\times2)$O/Ni(001) (dots). The spectral intensities were normalized at the 3*d* energy using procedure B (see Sec. III). The sample was demagnetized prior to data collection.

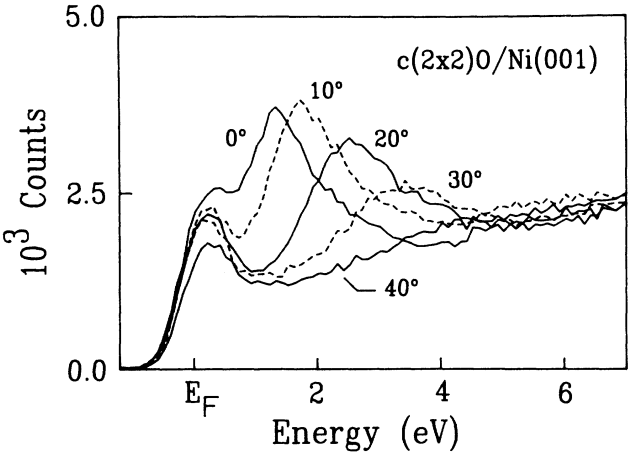

FIG. 10. The variation of $c(2\times2)$O/Ni(001) spin-integrated IP spectra with θ_e. The angle θ_e was varied in the (100) mirror plane (see Fig. 1). The spectral intensities were normalized using procedure A. The sample was demagnetized prior to data collection.

transition decreases in intensity with θ_e, but remains stationary in energy. Peaks 2 and 3 both disperse to higher energy, and lose intensity with increasing θ_e.

The intensity decrease observed in Fig. 9 at the energy of the 3*d* radiative transition 1 is in contradiction with the recent experiments of Scheidt *et al.*[14,15] Scheidt and co-workers report a 30% intensity *enhancement* of the 3*d* spectral intensity with 20 L oxygen exposure. This enhancement was attributed[14,15] to an oxygen-induced antibonding feature just above E_F at $\bar{\Gamma}'$. From the spin-dependent measurements, and the intensity variation shown in Fig. 9, we find little evidence for an oxygen-induced antibonding state above E_F at $\bar{\Gamma}'$ for $c(2\times2)$O/Ni(001). This state has been reported to possess Δ_5 symmetry.[17] Our photon-detection geometry is not optimal for the measurement of this group representation. However, Δ_5-symmetry states are to some extent detectable, as indicated by the observation of the Δ_5-symmetry 3*d* band transition 1 on clean Ni(001).

A priori, one would not expect a bulklike transition to display the surface sensitivity exhibited by peak 2 in Fig. 9. For the inverse photoemission transition 2, the incident electron kinetic energy is ≈ 11 eV with respect to E_F. By extrapolation of existing inelastic mean-free-path (IMFP) measurements[47,48] for Ni, we estimate the IMFP of the incident electrons responsible for peak 2 to be ≈ 6 Å or ≈ 5 atomic layers. Scheidt and co-workers[14] attributed the adsorbate-induced decrease in the peak-2 intensity to strong electronic rearrangements in the surface region of Ni(001) that destroy the coupling conditions in the initial state between the vacuum-free electrons and the initial state within the Ni solid. However, if the spectral transitions 1 and 2 both originate from the same initial state, then one would also expect this breakdown in the coupling conditions to lead to the same decrease in the intensity of the 3*d* transition 1. Such a large decrease is not observed. A bulk transition can theoretically[49] have a small IMFP if the transition takes place near a Brillouin-zone boundary. Again one would then expect an analogous sensitivity for the 3*d* transition 1, which is not observed.

Surface umklapping could be responsible for differential adsorbate-induced intensity decreases of bulklike transitions. Surface umklapping is the term applied to the variation of an electron wave-vector by a surface reciprocal-lattice vector $g_{\parallel}$. When these $g_{\parallel}$ are small, as is the case with a large real-space adsorbate unit cell such as $c(2\times2)$, the umklapp effect can dramatically alter spectral intensities in angle-resolved photoemission spectra.[50] Surface umklapping could in principle affect inverse photoemission spectra. However, Fig. 11 shows that the 4*sp* band sharply decreases in intensity with only a 3 L oxygen exposure. This exposure produces an oxygen coverage of ≈ 0.3 monolayers. Since the normal Ni(001) LEED pattern $[p(1\times1)]$ is still observed at this exposure, surface umklapping cannot explain the extreme surface sensitivity of the spectral transition 2.

We are left with final-state explanations for the surface sensitivity of peak 2. One could assign the phenomenon to a significant alteration of the Ni 4*sp* electronic structure in the near-surface layers of Ni upon chemisorption. It will be seen in Fig. 12 that a $c(2\times2)$ sulfur overlayer almost completely removes the spectral peak 2. This suggests that a chemisorption-induced disruption of the near-surface electronic structure would have to be exceptionally strong and delocalized over the ≈ 6 Å depth sensitivity of the IP measurement. This scenario, though possible, seems unlikely.

It has been theoretically predicted[34,35] that an $n=0$ crystal-induced unoccupied surface state should be

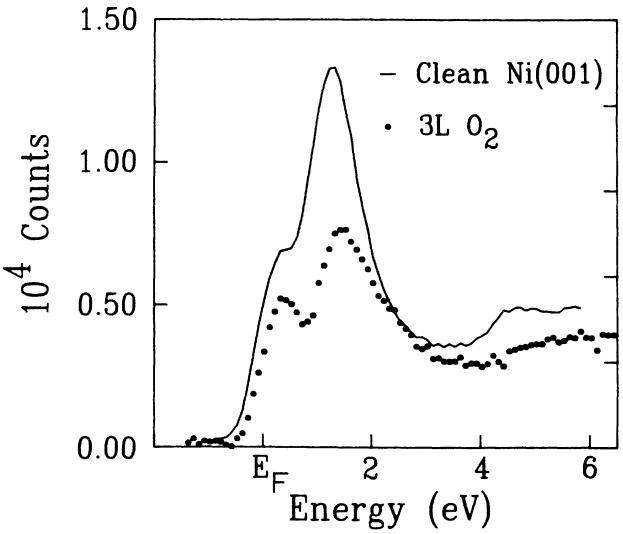

FIG. 11. A comparison of normal incidence ($\theta_e=0°$) spin-integrated IP spectra of clean Ni(001) (solid line) and Ni(001) exposed to 3 L of oxygen (dots). The spectral intensities were normalized at the 3*d* energy using procedure B.

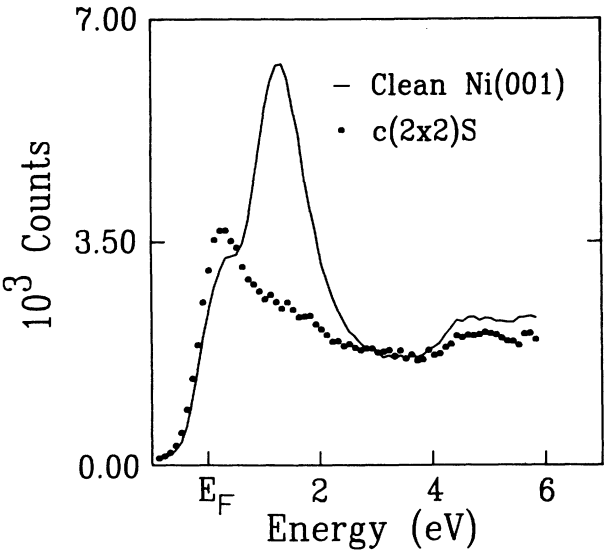

FIG. 12. A comparison of normal incidence ($\theta_e = 0°$) spin-integrated IP spectra of clean Ni(001) (solid line) and $c(2\times2)$S/Ni(001) (dots). The spectral intensities were normalized at the 3*d* energy using procedure B. The sample was demagnetized prior to data collection.

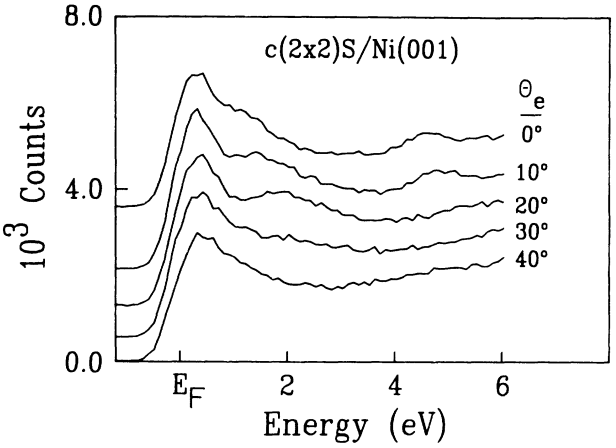

FIG. 13. The variation of $c(2\times2)$S/Ni(001) spin-integrated IP spectral with θ_e. The angle θ_e was varied in the (100) mirror plane (see Fig. 1). The sample was demagnetized prior to data collection. The spectra have been first normalized using procedure A, and then rigidly shifted in intensity to clarify the presentation.

present on Ni(001) at the $\bar{\Gamma}$ point of the SBZ and that this state should have nearly the same dispersion relations as the Ni 4*sp* band. If the spectral intensity of this surface state were significantly larger than that of the 4*sp* band, the surface sensitivity of transition 2 could be easily explained as the quenching of an unresolved surface state. We feel that this surface state scenario is quite consistent with the existing data, and we tentatively interpret the spectral peak 2 as radiative transitions into both a Ni 4*sp* band and an $n=0$ surface state.

One might have expected that a chemisorbed oxygen layer would decrease the magnetization of the surface and perhaps the near-surface layers of Ni(001), and therefore decrease the spin dependence of the IP spectra. It is important to note that the ARSPIPES spectra are generated by very low energy electrons. For the 3*d* radiative transition 1, the incident electron kinetic energy is ≈ 10 eV with respect to the nickel Fermi level. From existing inelastic mean-free-path (IMFP) measurements[47,48] for Ni, we estimate the IMFP of an incident 10 eV electron to be ≈ 6 Å. Despite this level of surface sensitivity, the spin asymmetry of the 3*d* spectral peak 1 displays little variation with $c(2\times2)$ oxygen chemisorption. This suggests that *any magnetization decrease induced by oxygen is probably confined to the surface layer.*

VI. RESULTS AND DISCUSSION: $c(2\times2)$S/Ni(001)

The geometric structure of $c(2\times2)$S/Ni(001) has been much less controversial than for oxygen.[27,28] For sulfur, only a single, well-defined $c(2\times2)$ chemisorption phase exists at half-monolayer coverage. Figure 12 presents a comparison of normal incidence IP spectra of clean Ni(001) (solid line) and $c(2\times2)$S/Ni(001) (dots). These spectra have been normalized at the 3*d* energy by procedure B. Note the almost complete disappearance of the spectral peak 2. Again, this surface sensitivity is very surprising for a bulk transition, and indirectly suggests that peak 2 involves transitions into an unresolved crystal-induced unoccupied surface state at $\bar{\Gamma}$ on clean Ni(001). In contrast with the $c(2\times2)$O results, we observe an increase of the intensity at the 3*d* feature 1. This enhancement is accompanied by *a fourfold decrease of the spin asymmetry at the 3d energy to −2(2)%.* This asymmetry variation is in marked contrast to the results for oxygen chemisorption that produced an insignificant variation in the feature-1 spin asymmetry.

We attribute the intensity enhancement at peak 1 to a sulfur-induced antibonding state at $\bar{\Gamma}'$ in the $c(2\times2)$ SBZ. If this assignment is correct, then the fourfold decrease in spin asymmetry indicates that this state would be primarily of *majority-spin character.* Since the spectral composition of the intensity at the 3*d* energy is changing, the chemisorption-induced magnetization disruption could be confined to the surface layer and still produce the observed dramatic decrease in the spin asymmetry. Recent spin-resolved calculations[29] for the $c(2\times2)$S/Ni(001) electronic structure do not, however, predict a sulfur-induced unoccupied electronic state at $\bar{\Gamma}'$.

The surface feature 3 shows an interesting response to sulfur chemisorption. In contrast to the behavior observed for oxygen chemisorption, the image-potential state energy is remarkably unaffected by the presence of a $c(2\times2)$ sulfur overlayer. This lack of energy shift is surprising. Work function variations were not monitored in the present investigation. However, the Ni(001) work function is reported[45] to increase by 0.38 eV with $c(2\times2)$ sulfur chemisorption. If true, then the IP re-

sults suggest that *changes in the energy of the Ni(001) image-potential state cannot be predicted from adsorbate-induced variations in the work function.* The variations of the $c(2\times2)$S/Ni(001) spectra with θ_e are shown in Fig. 13.

VII. CONCLUSIONS

An ARSPIPES study of Ni(001) revealed spectral transitions that were in good agreement with previous work. "Bulklike" spectral peaks could be readily assigned to $k_\perp$-conserving radiative transitions between a free-electron initial-state band and theoretical bulk final states. A minority-spin character was observed for a radiative transition into the unoccupied Ni $3d$ band. No definitive spin dependence was found for transitions into the unoccupied $4sp$ band, a potentially unresolved crystal-induced surface state, or an image-potential surface state.

The presence of a chemisorbed $c(2\times2)$ oxygen overlayer does not appreciably affect the spin dependence or the intensity of the Ni $3d$ IP transition. Little evidence is found for an oxygen-induced state above the Fermi level at $\bar{\Gamma}'$ in contrast with previous work.[14,15] The persistent spin asymmetry for the $3d$ transition suggests that a magnetization decrease induced by oxygen, if present, is probably confined to the Ni(001) surface layer.

A $c(2\times2)$ sulfur overlayer almost completely quenches the radiative transition previously assigned to the Ni $4sp$ band. The sensitivity of this transition to both chemisorbed oxygen and sulfur provides indirect evidence for the coexistence of an intense unresolved $n=0$ image-potential surface state. In contrast to $c(2\times2)$ oxygen chemisorption, sulfur increases the spectral intensity, and drastically decreases the spin asymmetry at the $3d$ transition 1. This finding probably results from the presence of a sulfur-induced majority-spin unoccupied state at $\bar{\Gamma}'$. The energy of the image-potential state remains fixed upon sulfur chemisorption, even though $c(2\times2)$S reportedly[45] causes a 0.38 eV increase in the work function. This behavior is in contrast with that observed for $c(2\times2)$O/Ni(001), and indicates that the energy of the Ni image-potential state need not reflect adsorbate-induced variations in the Ni(001) work function.

ACKNOWLEDGMENTS

The authors thank Professor J. Callaway and G. Fuster for providing a listing of their theoretical Ni band structure. Helpful discussions with N. V. Smith, P. D. Johnson, Th. Fauster, V. Dose, C. S. Fadley, R. L. Richards, D. R. Penn, J. W. Gadzuk, S. Chubb, and C. L. Fu are greatly appreciated. This work was supported in part by the U. S. Office of Naval Research.

*Present address: Department of Chemistry, Lehigh University, Bethlehem, PA 18015.

[1]G. Allan, in *Handbook of Surfaces and Interfaces,* edited by L. Dobrzynski (Garland STPM, New York, 1978), Vol. 1, p. 299.

[2]F. Herman and S. Skillman, *Atomic Structure Calculations* (Prentice-Hall, Englewood Cliffs, New Jersey, 1963).

[3]N. Mårtensson and B. Johansson, Phys. Rev. Lett. **45**, 482 (1980).

[4]D. R. Penn, Phys. Rev. Lett. **42**, 921 (1979).

[5]L. A. Feldkamp and L. C. Davis, Phys. Rev. B **22**, 3644 (1980).

[6]S. Hüfner and G. W. Wertheim, Phys. Lett. **51A**, 301 (1975).

[7]C. Guillot, Y. Ballu, J. Paigne, J. Lecante, K. P. Jain, P. Thiry, R. Pinchaux, Y. Petroff, and L. M. Falicov, Phys. Rev. Lett. **39**, 1632 (1977).

[8]J. Unguris, A. Seiler, R. J. Celotta, D. T. Pierce, P. D. Johnson, and N. V. Smith, Phys. Rev. Lett. **49**, 1047 (1982).

[9]C. S. Feigerle, A. Seiler, J. L. Pena, R. J. Celotta, and D. T. Pierce, Phys. Rev. Lett. **56**, 2207 (1986).

[10]A. Seiler, C. S. Feigerle, J. L. Pena, R. J. Celotta, and D. T. Pierce, Phys. Rev. B **32**, 7776 (1985).

[11]A. Goldmann, M. Donath, W. Altmann, and V. Dose, Phys. Rev. B **32**, 837 (1985).

[12]D. P. Woodruff, N. V. Smith, P. D. Johnson, and W. A. Royer, Phys. Rev. B **26**, 2943 (1982).

[13]K. Desinger, V. Dose, M. Globl, and H. Scheidt, Solid State Commun. **49**, 479 (1984).

[14]H. Scheidt, M. Globl, and V. Dose, Surf. Sci. Lett. **123**, L728 (1982).

[15]V. Dose, M. Globl, and H. Scheidt, J. Vac. Sci. Technol. **A1**, 1115 (1983).

[16]W. Altmann, K. Desinger, M. Donath, V. Dose, A. Goldmann, and H. Scheidt, Surf. Sci. **151**, L185 (1985).

[17]K. Desinger, V. Dose, A. Goldmann, W. Jacob, and H. Scheidt, Surf. Sci. **154**, 695 (1985).

[18]For a review, see C. R. Brundle and J. Q. Broughton, in *The Chemical Physics of Solid Surfaces and Heterogeneous Catalysis,* edited by D. A. King and D. P. Woodruff (Elsevier, Amsterdam, in press), Vol. 3.

[19]S. Mukherjee, V. Kumar, and K. H. Bennemann, Surf. Sci. Lett. **167**, L210 (1986).

[20]R. W. Godby, G. A. Benesh, R. Haydock, and V. Heine, Phys. Rev. B **32**, 655 (1985).

[21]M. C. Desjonqueres and F. Cyrot-Lackmann, Surf. Sci. **80**, 208 (1979).

[22]C. S. Wang and A. J. Freeman, Phys. Rev. B **19**, 4930 (1979).

[23]S. R. Chubb and A. J. Freeman (unpublished).

[24]J. M. Gallagher and R. Haydock, Surf. Sci. **83**, 117 (1979).

[25]A. Liebsch, Phys. Rev. B **17**, 1653 (1978).

[26]D. W. Bullett and M. L. Cohen, J. Phys. C **10**, 2101 (1977).

[27]J. J. Barton, C. C. Bahr, Z. Hussain, S. W. Robey, J. G. Tobin, L. E. Klebanoff, and D. A. Shirley, Phys. Rev. Lett. **51**, 272 (1983).

[28]S. Brennan, J. Stohr, and R. Jaeger, Phys. Rev. B **24**, 4871 (1981).

[29]C. L. Fu and A. J. Freeman (unpublished).

[30]E. W. Plummer, B. Tonner, N. Holzwarth, and A. Liebsch, Phys. Rev. B **21**, 4306 (1980).

[31]P. L. Cao, D. E. Ellis, and A. J. Freeman, Phys. Rev. B **25**,

2124 (1982).
[32]D. T. Pierce, R. J. Celotta, G. C. Wang, W. N. Unertl, A. Galejs, C. E. Kuyatt, and S. R. Mielczarek, Rev. Sci. Instrum. **51**, 478 (1980).
[33]G. Denninger, V. Dose, and H. Scheidt, Appl. Phys. **18**, 375 (1979).
[34]R. F. Garrett and N. V. Smith, Phys. Rev. B **33**, 3740 (1986).
[35]A. Goldmann, V. Dose, and G. Borstel, Phys. Rev. B **32**, 1971 (1985).
[36]D. W. Jepsen, F. J. Himpsel, and D. E. Eastman, Phys. Rev. B **26**, 4039 (1982).
[37]G. Fuster and J. Callaway (private communication).
[38]See, for example, L. E. Klebanoff, S. W. Robey, G. Liu, and D. A. Shirley, Phys. Rev. B **31**, 6379 (1985).
[39]W. Eberhardt and E. W. Plummer, Phys. Rev. B **21**, 3245 (1980).
[40]P. D. Johnson and N. V. Smith, Phys. Rev. B **27**, 2527 (1983).
[41]S. L. Hulbert, P. D. Johnson, N. G. Stoffel, W. A. Royer, and N. V. Smith, Phys. Rev. B **31**, 6815 (1985).
[42]N. V. Smith, Appl. Surf. Sci. **22/23**, 349 (1985).
[43]D. T. Pierce, in *Magnetic Properties of Low Dimensional Systems,* edited by L. M. Falicov and J. L. Moran-Lopez (Springer-Verlag, Berlin, 1986), p. 58.
[44]P. M. Echenique and J. B. Pendry, J. Phys. C **11**, 2065 (1978).
[45]J. E. Demuth and T. N. Rhodin, Surf. Sci. **45**, 249 (1974).
[46]V. Dose, W. Altmann, A. Goldmann, U. Kolac, and J. Rogozik, Phys. Rev. Lett. **52**, 1919 (1984).
[47]D. T. Pierce and H. C. Siegmann, Phys. Rev. B **9**, 4035 (1974).
[48]D. E. Eastman, in *Techniques of Metals Research,* edited by E. Passaglia (Interscience, New York, 1972), Vol. VI, part I, Chap. 6, p. 448.
[49]P. J. Feibelman and D. E. Eastman, Phys. Rev. B **10**, 4939 (1974).
[50]J. Anderson and G. J. Lapeyre, Phys. Rev. Lett. **36**, 376 (1976).